Progress In Electromagnetics Research Letters, Vol. 101, 117–125, 2021

Design and Measurement of Triple H-Slotted DGS Printed Antenna with Machine Learning

Mohammed F. Nakmouche[1, *], Abdemegeed M. M. A. Allam[2], Diaa E. Fawzy[3], and Mahmoud A. Abdalla[4]

Abstract—This paper presents the design and measurements of a dual-band Triple H-Defected Ground Structure (Triple H-DGS) antenna. DGS has proven to be successful in the design of multiband antennas; however because of the lack of a standard approach, the determination of the exact position of the Triple H-DGS requires rigorous and lengthy numerical computations. The aim of the current work is to present a state-of-the-art innovative, efficient, and accurate solution based on Machine Learning (ML) techniques. The design is based on Substrate Integrated Waveguide (SIW) technology which provides low cost, small size, and convenient integration with planar circuits. The antenna is fabricated on a Roger 5880 substrate with a thickness of 1.6 mm, relative dielectric constant of 2.2, and tangent loss of 0.0009. The proposed antenna was developed using a hybrid solution based on CST Microwave Studio assisted by ML, and the fabricated prototype was measured using both ROHDE & SCHWARZ ZVB20 network analyser and an anechoic chamber setting. The measurement results show good agreement with the simulation. The antenna demonstrates a dual-band performance at centre frequencies of 12.67 GHz and 14.56 GHz, for which the respective antenna gains are 7.03 dBi and 7.38 dBi, and antenna directivities of 7.77 dB and 8.13 dB, respectively. The antenna total efficiencies are 95.25% and 95.60%, at the corresponding centre frequencies. The developed ML based technique shows good accuracies of about 98% in the determination of the DGS position and saves more than 99% of the computational time. The developed antenna is compact, simple in structure, and can be used for different applications in the Ku band.

1. INTRODUCTION

The advancements in the microstrip antenna design technologies and techniques have been the key success factors in developing new promising wireless applications [1, 2], where size and ease of installation are vital considerations. However, antenna bandwidth and efficiency have deteriorated in many of the newly proposed antenna designs [3–6]. Several methods have been implemented to modify the antenna design in a way that alleviates such drawbacks [7]. This is achieved by adopting different feeding techniques, including microstrip line, coaxial probe, aperture coupling, and proximity [8].

Patch antenna designs can be altered in a way that makes them appropriate for multi-band wireless communications including multi-layer rectangular patch antenna array [9–12], a low-profile dual-band circular polarized antenna for a nanosatellite communication system [13], and multi-layered based on metasurface dual circularly polarized (CP) patch antenna [14] achieving a broadband operating frequency band. The main drawbacks of the aforementioned designs are the difficulty of their fabrication due to the air gap between layers and some alignment issues. Furthermore, using the coaxial feeding technique makes the design unsuitable for integrated circuit configuration and incompatible for the

Received 5 September 2021, Accepted 1 December 2021, Scheduled 14 December 2021

* Corresponding author: Mohammed Farouk Nakmouche (Nakmouche.MFarouk@gmail.com).

[1] Faculty of Engineering, İzmir University of Economics, Izmir, Turkey. [2] Department of Communication Engineering, German University in Cairo, Cairo, Egypt. [3] Electronic Engineering Department, Military Technical College (MTC), Cairo, Egypt.

use as a planar antenna. Alternatively, the use of Defected Ground Structures (DGSs) has proven to be a successful method for obtaining multiband resonances through current disturbances created on the surface of the structure. This technique has been used in the filter design and in antennas development [15–23].

This paper presents a novel technique to address the lack of a standard approach for determining the exact position of a slotted Triple H-DGS in regard to particular resonance frequencies by providing an innovative, efficient, and accurate solution based on Machine Learning. The current paper is structured as follows. The first part presents the proposed antenna design. The following sections concentrate on the optimization of the position of a Triple-HDGS to achieve the required resonance frequencies of the antenna and with the use of our proposed machine learning based approach. Besides, the fabrication and measurement of the Triple-HDGS antenna for the aim to validate our proposed approach are conducted. The fabricated antenna is then measured on ROHDE & SCHWARZ ZVB20 network analyser for the return loss and a chamber setting for the radiation parameters.

2. ANTENNA DESIGN

Figures 1 and 2 present the SIW geometry, the Triple-HDGS unit cell which is found to be optimum with respect to the required resonance bands based on our previous study in [16], and the overall proposed antenna structure, respectively. Table 1 depicts all dimensions. Figure 3 shows the fabricated antenna. The developed antenna is based on Roger/Duroid5880 (relative permittivity and loss tangent of 2.2 and 0.0009, respectively) and a thickness of $H_{sub} = 1.6\,\text{mm}$ for the substrate material.

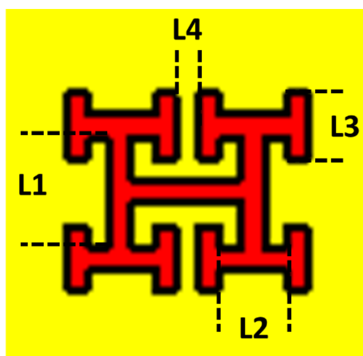

Figure 1. The geometry of H-DGS unit cell.

Table 1. Design parameters of the proposed antenna.

Variables	**A**	**B**	**AA**	**BB**	**Af**	**G2**	**G3**	**P**	**d**	**L1**	**Af**
Value (mm)	45.5	37	19	23	31	7	8.6	0.75	0.4	3	31
Variables	**Bf**	**As**	**Wg**	**Wf**	**G1**	**L1**	**L2**	**L3**	**L4**	**G1**	**Hsub**
Value (mm)	5	1.6	17	1.75	4.5	3	1.5	1.5	0.5	4.5	1.6

3. MACHINE LEARNING AND EXPERIMENTAL RESULTS

With the aim of automating the design of a dual-band antenna using DGS based technology, Artificial Neural Network (ANN) modelling is used. The motivation behind to use ANN for the prediction of the optimal position of Triple H-DGS is the lack of a standard approach that can be used to determine the exact position of any DGS geometry in regard to a particular resonance frequency [24, 25]. The position of the Triple H-slotted DGS controls the resonance frequencies in terms of dual or a single resonance.

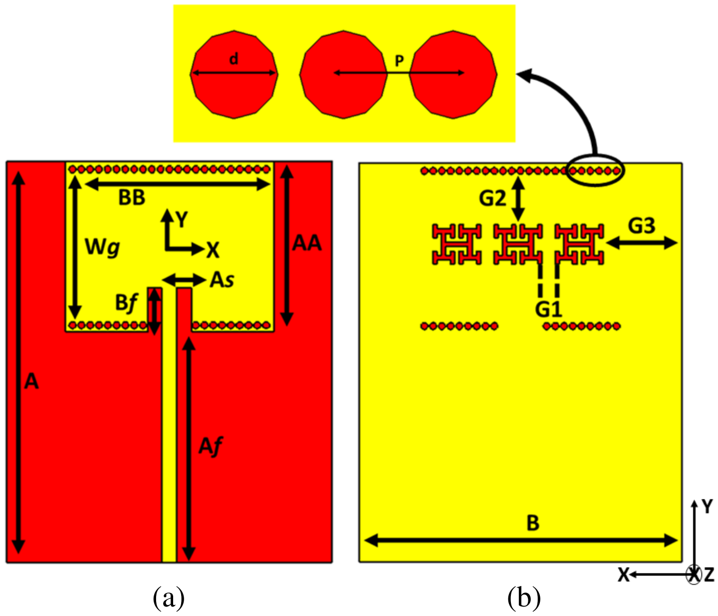

Figure 2. Schematic diagram of the proposed antenna. (a) Top view. (b) Bottom view.

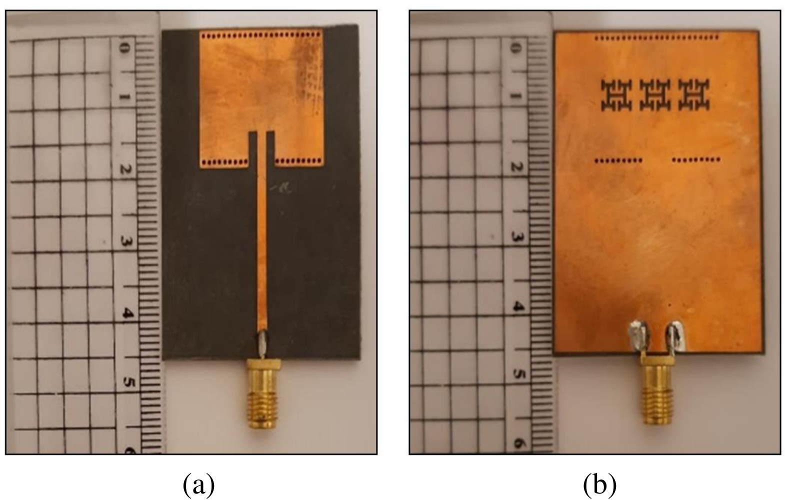

Figure 3. Unit cell of the H shaped DGS. (a) Top view. (b) Bottom view.

The ANN based model is developed using a MATLAB code to produce resonance frequencies and return losses (S_{11}) as output parameters with the consideration of the position values of the Triple H-slotted DGS as input (X pos & Y pos). These values should be within the patch ground plane limits. Table 2 lists the results obtained from both the CST and ANN simulations in terms of X, Y positions, resonance frequencies, and return losses (S_{11}). Figure 5 depicts that an optimal return loss is obtained when the position of the DGS is at the centre of the ground plane.

In order to validate our developed ANN model, the mean square error (MSE) using Equation (1) [26] is calculated and reported in Table 3.

$$\text{RMSE} = \sqrt{\frac{1}{n}\sum_{i=1}^{n}(t_i - \alpha_i)^2} \tag{1}$$

where n is the total number of samples, and t_i and α_i represent the target and output data, respectively.

Table 2. A comparison between the obtained ANN and simulated CST results.

		Input		Targets (Simulated by CST)		Outputs (Estimated by ANN)	
		X Position	Y Position	Freq (GHz)	S_{11} (dB)	Freq (GHz)	S_{11} (dB)
Training Data	**01**	−2	1	13 14.1	12 15.66	12.98 14	11.97 15.59
	02	−2	−2	13.7	20.6	13.25	20.4
	...	...	...	...	...	...	...
	...	...	...	...	...	...	...
	74	−1	1	14.36	25.2	14.38	24.98
	75	−1	0	11.34	28.5	11.32	28.47
Validation Data	**76**	0	1	12.7 14.4	12.1 11.5	12.68 14.38	11.98 11.48
	77	1	0	12.5	22	12.37	21.9
	...	...	...	...	...	...	...
	...	...	...	...	...	...	...
	89	−1	−2	14.38	24.08	14.35	24.06
	90	1	1	12.5	45.6	12.47	45.72
Testing Data	**91**	0	−1	12.7 14.4	14.8 11.6	12.68 14.37	14.77 11.57
	92	0	0	14.56 12.6	14.52 18.1	14.53 12.58	14.5 17.89
	...	...	...	...	...	...	...
	...	...	...	...	...	...	...
	99	1	−2	12.48	27.3	12.52	27
	100	1	−1	12.5	28	12.47	27.89

Table 3. Mean Square Error (MSE) for our developed ANN model.

Design Parameters	Mean Square Error (MSE)			
	Freq 01 (GHz)	S_{11} (dB)	Freq 02 (GHz)	S_{11} (dB)
Optimal X & Y Position	0.0662	0.0287	0.0099	0.0208

The testing error is represented as a function of Regression R-value (R-value close to 1 means that the ANN model is well trained, tested, and validated) [27] as shown in Figure 4, respectively. From the calculated MSE, extracted R-value graphs, we can notice that our developed ANN model has a good performance. Lastly, there is a save of about 99% of the computational time while maintaining a prediction error below 2%.

As an experimental validation, Figure 6 compares the reflection coefficient values obtained from simulation with those obtained from measurement. It is found that the proposed antenna has two resonance frequencies at 12.58 GHz and 14.64 GHz frequencies with bandwidths of 100 MHz and 230 MHz at the two frequencies, respectively. From Figure 7, it can be noticed that the gains at the two frequencies 12.67 and 14.56 are 7.03 dB and 7.38 dBi. The proposed antenna achieved radiation efficiencies of about 95.25% and 95.60% at 12.67 GHz and 14.56 GHz, respectively as displayed in Figure 7. Lastly, the radiation patterns at H and E planes are sketched in Figure 8. One notices that the maximum radiation is observed to be at 0° degrees. One can also notice the slight differences between the simulated and measured results, which are introduced by the SMA connectors and the environment in which the measurements are conducted.

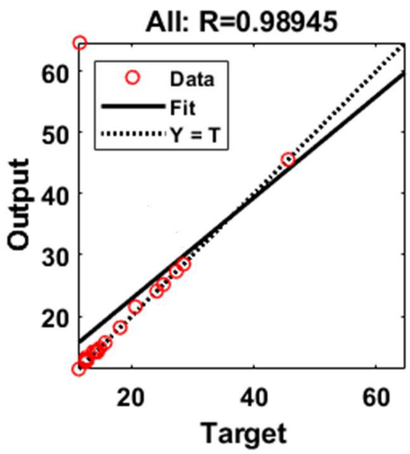

Figure 4. Regression R-values.

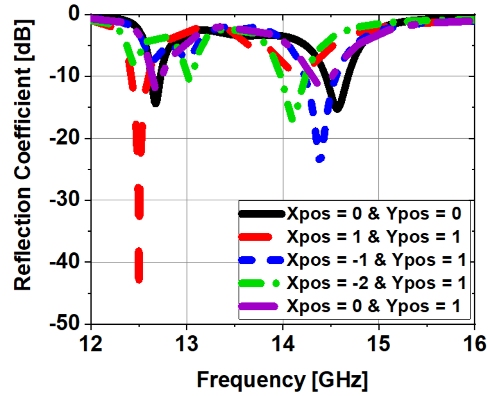

Figure 5. Simulated reflection coefficients for different X pos & Y pos values.

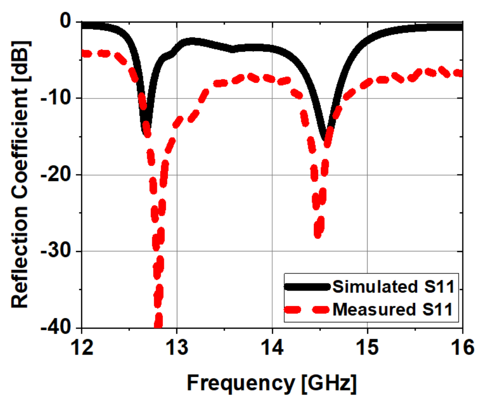

(a)

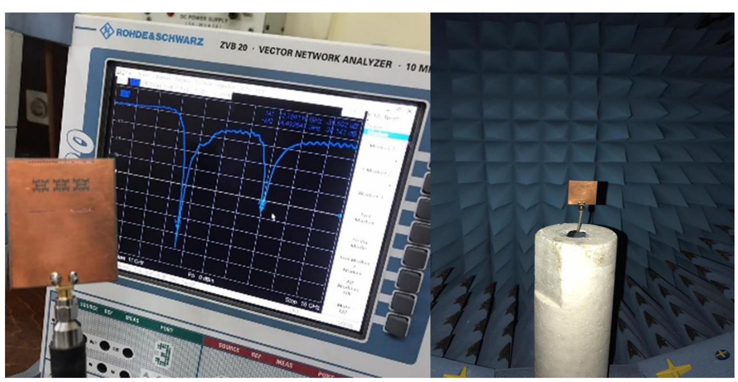

(b)

Figure 6. Simulated and measured results. (a) Reflection coefficients. (b) Setup of network analyser and anechoic chamber.

The surface current distributions at 12.67 GHz and 14.56 are shown in Figures 9(a) and (b). It can be noticed that the surface currents are mainly distributed around the Triple H-DGS slotted in the ground layer and the vias placed in the top and bottom. Thus, the dual-band response is mainly caused by the Triple H-DGS.

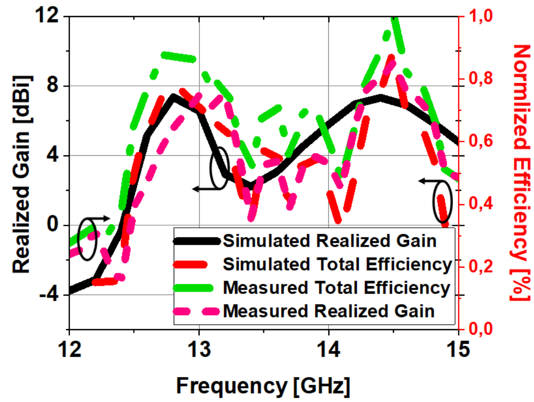

Figure 7. Simulated and measured realized gain & antenna efficiency.

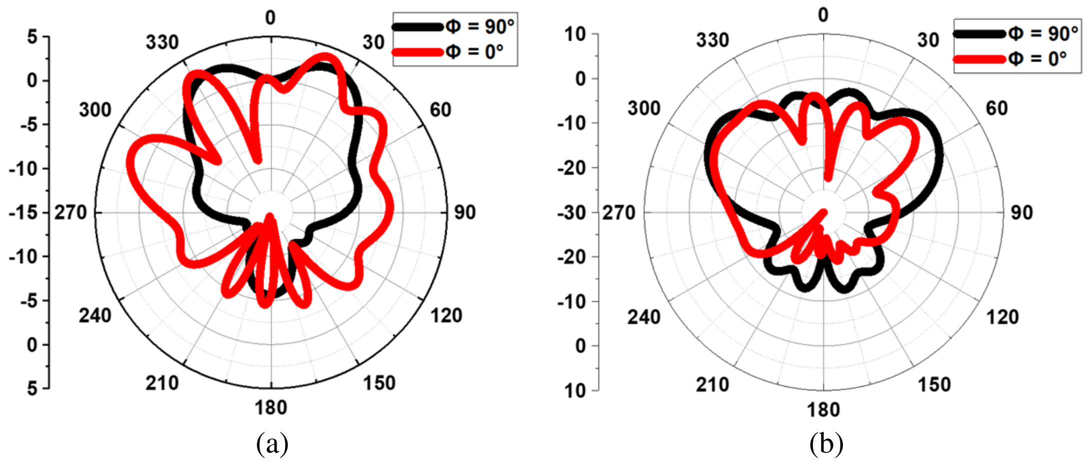

Figure 8. Simulated radiation patterns (a) at 12.67 GHz, (d) at 14.56 GHz.

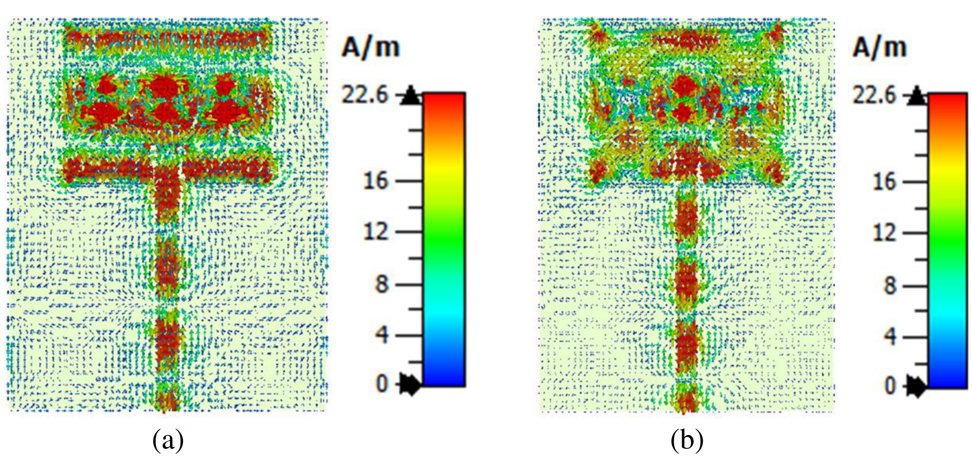

Figure 9. Surface current distribution (a) at 12.67 GHz, (b) at 14.56 GHz.

A quantitative comparison is made with other similar reported studies in the literature [24–28] and listed in Table 4. Our developed antenna with ML has a higher realized gain over [24–27] yet having a lower antenna dimension. However, whereas the work presented in [28] shows a slightly higher gain, our suggested antenna has a superior lower dimension.

Table 4. Comparison with previous semilar antennas.

References	Frequency Bandwidth (GHz)	Gain (dB)	Radiation Efficiency	Dimension
Ref. [28]	**2.7** **11**	**1.1** **6**	**NA**	**40.7 × 34.2**
Ref. [29]	**16** **30**	**6.9** **5.9**	**NA**	**8 × 8**
Ref. [30]	**3.5** **5.8**	**10.2** **8.94**	**NA**	**95 × 65**
Ref. [31]	**3.5** **5.2**	**1.07** **2.96**	**NA**	**15 × 25**
Ref. [32] (Reconfigurable)	**Case 01: 4.75 5.05** **Case 02: 5.11 5.18**	**6.82**	**NA**	**15 × 25**
Our Antenna	**12.67** **14.56**	**7.03** **7.38**	**95.25** **95.60**	**19 × 23**

4. CONCLUSION

The current study presents a novel machine learning based technique to accelerate the development of DGS-based patch antennas. The motivation behind this work is the lack of a standard approach for determining the exact position of a DGS in regard to a particular resonance frequency. The current approach considers the development of a patch antenna based on SIW Triple H-slotted DGS geometry. The proposed design is fabricated on a Roger 5880 substrate with a thickness of 1.6 mm, relative dielectric constant of 2.2, and tangent loss of 0.0009. The obtained results show a dual-band behaviour at 12.67 GHz and 14.56 GHz frequencies with gains of 7.03 dBi and 7.38 dBi, respectively. The antenna's total efficiencies are 95.25% and 95.60% at the two frequencies. The ML-based approach predicts the position of the DGS with the accuracy of about 98%.

REFERENCES

1. Balanis, C. A., *Antenna Theory Analysis and Design*, 4th Edition, Wiley, 2016.
2. Garg, R., P. Bartia, I. Bahl, and A. Ittipiboon, *Microstrip Antenna Design Handbook*, Artech House Inc., 2001.
3. Ali, W., E. Hamad, M. Bassiuny, and M. Hamdallah, "Complementary split ring resonator based triple band microstrip antenna for WLAN/WiMAX applications," *Radioengineering*, Vol. 26, No. 1, 78–84, 2017.
4. Saroj, A. K., M. G. Siddiqui, M. Kumar, and J. Ansari, "Design of multiband quad-rectangular shaped microstrip antenna for wireless applications," *Progress In Electromagnetics Research M*, Vol. 59, 213–221, 2017.
5. Fertas, F., M. Challal, and K. Fertas, "Miniaturized quintuple band antenna for multiband applications," *Progress In Electromagnetics Research M*, Vol. 89, 83–92, 2020.

6. Singh, A. K., M. P. Abegaonkar, and S. K. Koul, "Miniaturized multiband microstrip patch antenna using metamaterial loading for wireless application," *Progress In Electromagnetics Research C*, Vol. 83, 71–82, 2018.
7. Saini, G. S. and R. Kumar, "A low profile patch antenna for Ku-band applications," *Int. J. Electron. Lett.*, 1–11, 2019.
8. Vijayvergiya, P. L. and R. K. Panigrahi, "Single-layer single-patch dual band antenna for satellite applications," *IET Microwaves, Antennas Propag.*, Vol. 11, No. 5, 664–669, 2017.
9. Hassan, M. M., M. Hussain, A. A. Khan, I. Rashid, and F. A. Bhatti, "Dual-band B-shaped antenna array for satellite applications," *Int. J. Microw. Wirel. Technol.*, November 2020.
10. Mener, S., R. Gillard, and L. Roy, "A dual-band dual-circular-polarization antenna for Ka-band satellite communications," *IEEE Antennas Wirel. Propag. Lett.*, Vol. 16, 274–277, 2017.
11. Mao, X., S. Gao, Y. Wang, and J. T. Sri Sumantyo, "Compact broadband dual-sense circularly polarized microstrip antenna/array with enhanced isolation," *IEEE Trans. Antennas Propag.*, Vol. 65, No. 12, 7073–7082, 2017.
12. Swetha, A. and K. R. Naidu, "Miniaturized antenna using DGS and meander structure for dual-band application," *Microw. Opt. Technol. Lett.*, Vol. 62, No. 11, 3556–3563, 2020.
13. Alam, T. and M. T. Islam, "A dual-band antenna with dual-circular polarization for nanosatellite payload application," *IEEE Access*, Vol. 6, 78521–78529, 2018.
14. Wu, J., Y. J. Cheng, H. Bin Wang, Y. C. Zhong, D. Ma, and Y. Fan, "A wideband dual circularly polarized full-corporate waveguide array antenna fed by triple-resonant cavities," *IEEE Trans. Antennas Propag.*, Vol. 65, No. 4, 2135–2139, 2017.
15. Ding, X., S. Wu, Z. Zhao, Z. Nie, and Q. H. Liu, "Meta-surface loading broadband and high-aperture efficiency dual circularly polarized patch antenna," *Int. J. RF Microw. Comput. Eng.*, March 2021.
16. Nakmouche, M. F., H. Taher, D. E. Fawzy, and A. M. M. A. Allam, "Development of a wideband substrate integrated waveguide bandpass filter using H-slotted DGS," *Proceedings — CAMA 2019: IEEE International Conference on Antenna Measurements and Applications*, 2019.
17. Zeng, J. and K. Luk, "A simple wideband magnetoelectric dipole antenna with a defected ground structure," *IEEE Antennas Wirel. Propag. Lett.*, Vol. 17, No. 8, 1497–1500, Aug. 2018.
18. Zhou, J., Y. Rao, D. Yang, H. J. Qian, and X. Luo, "Compact wideband BPF with wide stopband using substrate integrated defected ground structure," *IEEE Microwave and Wireless Components Letters*, Vol. 31, No. 4, 353–356, April 2021.
19. Han, C., D. Tang, Z. Deng, H. J. Qian, and X. Luo, "Filtering power divider with ultrawide stopband and wideband low radiation loss using substrate integrated defected ground structure," *IEEE Microwave and Wireless Components Letters*, Vol. 31, No. 2, 113–116, February 2021.
20. Nakmouche, M. F., A. M. M. A. Allam, D. E. Fawzy, and D. B. Lin, "Low profile dual band H-slotted DGS based antenna design using ANN for K/Ku band applications," *2021 8th Int. Conf. Electr. Electron. Eng., ICEEE 2021*, 2021.
21. Nakmouche, M. F., A. M. M. A. Allam, D. E. Fawzy, D. B. Lin, and M. Fathy Abo Sree, "Development of H-slotted DGS based dual band antenna using ANN for 5G applications," *15th Eur. Conf. Antennas Propag. (EuCap)*, 2021.
22. Kishore, N., G. Upadhyay, V. S. Tripathi, and A. Prakash, "Dual band rectangular patch antenna array with defected ground structure for ITS application," *AEU — Int. J. Electron. Commun.*, Vol. 96, 228–237, 2018.
23. Nakmouche, M. F. and M. Nassim, "Impact of metamaterials DGS in PIFA antennas for IoT terminals design," *The 6th International Conference on Image and Signal Processing and Their Applications*, November 2019.
24. El Misilmani, H. M., T. Naous, and S. K. Al Khatib, "A review on the design and optimization of antennas using machine learning algorithms and techniques," *Int. J. RF Microw. Comput. Eng.*, Vol. 30, No. 10, 2020.

25. Nakmouche, M. F., A. M. Allam, D. E. Fawzy, and D.-B. Lin, "Development of a high gain FSS reflector backed monopole antenna using machine learning for 5G applications," *Progress In Electromagnetics Research M*, Vol. 105, 183–194, 2021.
26. Sharma, K. and G. P. Pandey, "Efficient modelling of compact microstrip antenna using machine learning," *AEU — International Journal of Electronics and Communications*, Vol. 135, 153739, 2021, ISSN 1434-8411, https://doi.org/10.1016/j.aeue.2021.153739.
27. Sharma, Y., H. H. Zhang, and H. Xin, "Machine learning techniques for optimizing design of double T-shaped monopole antenna," *IEEE Trans. Antennas Propag.*, Vol. 68, No. 7, 5658–5663, July 2020, doi: 10.1109/TAP.2020.2966051.
28. Derbal, M. C., A. Zeghdoud, and M. Nedil, "A dual band notched UWB antenna with optimized DGS using genetic algorithm," *Progress In Electromagnetics Research Letters*, Vol. 88, 89–95, 2020.
29. Kandwal, A., "Compact dual band antenna design for Ku/Ka band applications," *AEM*, Vol. 6, No. 4, 1–5, October 2017.
30. Derbal, M. C. and M. Nedil, "A high gain dual band rectenna for RF energy harvesting applications," *Progress In Electromagnetics Research Letters*, Vol. 90, 29–36, 2020.
31. Thanki, P. and F. Raval, "I-shaped frequency and pattern reconfigurable antenna for WiMAX and WLAN applications," *Progress In Electromagnetics Research Letters*, Vol. 97, 149–156, 2021.
32. Saikia, B., P. Dutta, and K. Borah, "A compact dual asymmetric L-slot frequency reconfigurable microstrip patch antenna," *Progress In Electromagnetics Research C*, Vol. 113, 59–68, 2021.